Engineering the sub-Doppler force in magneto-optical traps

S. Xu,[*] P. Kaebert ⓘ, M. Stepanova, T. Poll, M. Siercke ⓘ,[†] and S. Ospelkaus
Institut für Quantenoptik, Leibniz Universität Hannover, 30167 Hannover, Germany

Current dual-frequency magneto-optical traps (MOTs) for ultracold molecules are plagued by sub-Doppler heating effects, making them vastly inferior to standard atomic MOTs. Here we demonstrate theoretically that the sub-Doppler effects in such a MOT can be engineered to provide cooling instead of heating. We give an intuitive picture how to achieve such cooling and show the cooling and trapping force results of the 16-level optical Bloch equations for the case of CaF molecules. From three-dimensional Monte Carlo simulations we estimate the temperature and density of our MOT to be $40\,\mu\mathrm{K}$ and $4 \times 10^8\,\mathrm{cm}^{-3}$, respectively, for a molecule number of 1×10^5. We also extend our idea to the case of atomic MOTs and show that it can be used to produce sub-Doppler forces in these systems that are much more robust against magnetic fields.

Magneto-optical trapping has been at the forefront of atomic and molecular cooling experiments for over three decades [1,2]. The technique is used in virtually every laboratory working with ultracold neutral particles, owing to the fact that it is able to capture, trap, and cool species down to temperatures inaccessible by any other nonoptical method. Once captured and cooled in a magneto-optical trap (MOT), other techniques, such as sub-Doppler cooling in molasses [3–8] and evaporative cooling [9–12] can be used to reduce temperatures and increase phase-space densities even further. Sub-Doppler mechanisms are, in fact, present even during the MOT stage. Their effect on MOT temperatures can be beneficial [13] or negligible [14] or, as is the case in current molecular MOTs, sub-Doppler effects can significantly increase MOT temperatures [15–18]. As such, the high temperatures and the resulting low MOT densities are significantly limiting the phase-space density of molecular systems. In this Letter, we propose experimental techniques to engineer these sub-Doppler effects. In particular we illustrate this by theoretically engineering a molecular magneto-optical trap for CaF where the sub-Doppler heating has been turned into sub-Doppler cooling. Monte Carlo simulations of the molecular cloud show a significant decrease in temperature and a consequential increase in density, which will have considerable impact on experiments using laser coolable molecules attempting to reach quantum degeneracy. Finally, we show how the same technique can be used to make sub-Doppler forces more robust against magnetic fields in atomic MOTs.

In a magneto-optical trap, particles are subjected to light from six laser beams, incident from six directions, as well as

*s.xu@iqo.uni-hannover.de
†siercke@iqo.uni-hannover.de

a quadrupole magnetic field. The purpose of the laser beams is twofold (1) their frequencies are tuned in such a way as to produce a velocity damping force on the particles, and (2) together with the magnetic field they produce a spatial restoring force. In the case of a type-I MOT operating on a $J \to J + 1$ transition [1] as is used to trap most atomic species, simply red detuning the lasers from resonance and choosing the correct circular polarizations ensures both damping and trapping. In the case of a molecular type-II MOT [19] operating on a $J \to J - 1$ transition, multiple laser frequencies, and polarizations must be used [15–18]. In both cases, the resulting photon scattering produces cooling and trapping. This stands in stark contrast to the forces responsible for sub-Doppler cooling/heating. Here, photon scattering serves the role of optical pumping, and the scattering itself is not the main contributor to the momentum change [4]. Rather, sub-Doppler processes generally rely on differential AC Stark shifts for slowing. Whereas the probability to scatter a photon scales as I/δ^2, where I is the laser intensity and δ is the laser detuning from resonance, the AC Stark shift scales as I/δ. This, then, highlights the idea behind this Letter: at least, to some degree, experiments should be able to control Doppler forces, relying on scattering, and sub-Doppler forces relying on the AC Stark shift, independently by adjusting laser intensity and detuning or adding additional lasers.

To illustrate this point we focus on the dual-frequency type-II MOTs currently used in ultracold molecule experiments. In particular, we focus on the case of CaF molecules. The ground state of CaF has a $F = 2$ level which couples to the $F' = 1$ level in the excited state (Fig. 1). Furthermore, the excited state g factor is small compared to that of the ground state. To produce a magnetic restoring force in such a system, two laser frequencies are necessary [Fig. 1(a)]: a red-detuned and a blue-detuned frequency as was first pointed out in Ref. [20]. For the beams traveling to the left (beams 3 and 4), the red-detuned beam is σ^- polarized and the blue-detuned beam is σ^+ polarized. When the molecules move to a region of higher field (to the right), the $m_F = \pm 2$ and $m_F = \pm 1$ levels shift closer to resonance with these beams [Fig. 1(b)].
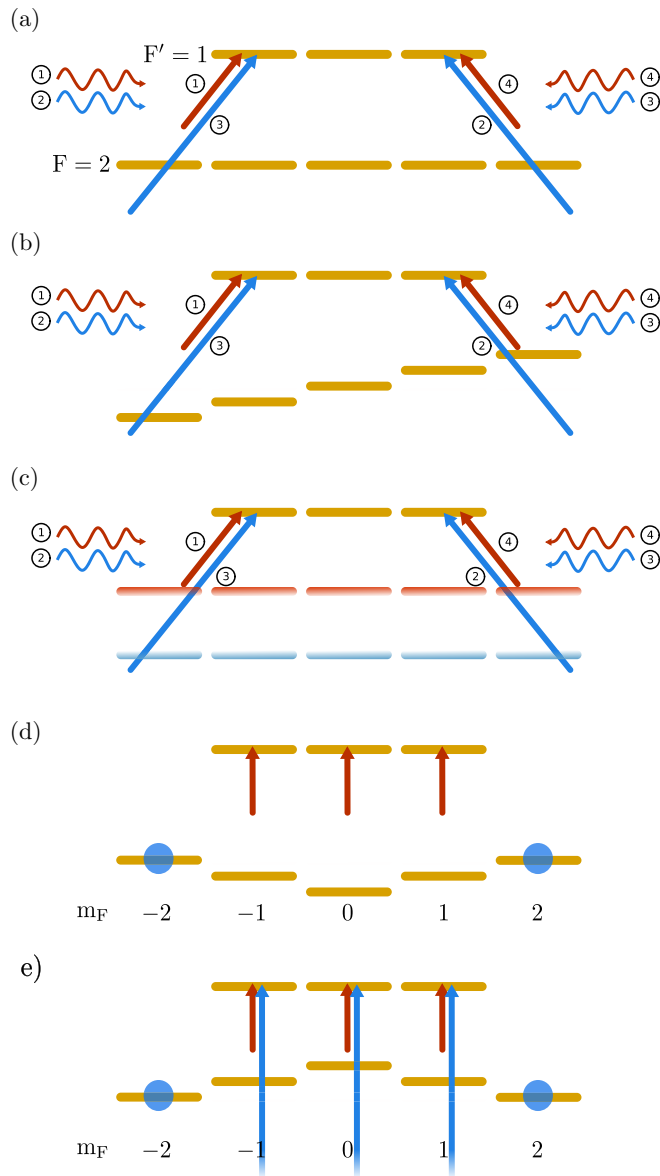
FIG. 1. The one-dimensional (1D) MOT laser configuration for a $F = 2$ to $F' = 1$ system. (a) Laser frequencies, directions, and polarizations needed. The four laser beams are labeled 1–4, respectively, with their colors representing their detuning and the horizontal direction of the straight arrows indicating their polarization. (b) In a positive magnetic field the ground-state Zeeman shift causes light to preferentially be scattered from beams 3 and 4, resulting in a momentum kick to the left. (c) Transitions as seen by the lasers for a molecule with a velocity to the right. Lasers 3 and 4 will see red-shifted transitions (red ground-state levels) whereas 1 and 2 see blue-shifted ones (blue ground-state levels). The overall laser detuning is chosen such that laser 4 comes into resonance sooner than laser 2, resulting in a damping force to the left. (d) AC Stark shift and optical pumping in red-detuned cork-screw molasses. (e) Adding a blue-detuned laser with the same polarization as the molasses laser can change the sign of the overall AC Stark shift, turning sub-Doppler heating into cooling.

Conversely, the beams propagating to the right are shifted out of resonance, and the resulting photon-scattering imbalance pushes molecules towards the center of the quadrupole field.

If the detuning of the red- and blue-detuned laser components is equal but opposite, there is no velocity-dependent force: when a molecule travels towards one of the laser beam pairs it scatters more photons from the counterpropagating red-detuned beam, but it also scatters more photons from the blue-detuned co-propagating beam. To get a velocity-damping force in this system then, both frequency components need to be shifted slightly higher so that the red-detuned component is closer to resonance than the blue-detuned one. This ensures that molecules preferentially scatter photons from the counterpropagating laser beams [Fig. 1(c)].

The laser configuration producing the dual-frequency MOT force brings with it an unfortunate consequence: near zero velocity at the trap center the red-detuned laser beams are closer to resonance than the blue-detuned ones. This results in AC Stark shifts that lower the energy of the ground states by an amount depending on the coupling strength. In 1D, the counterpropagating red-detuned σ^+ and σ^- laser beams form a corkscrew polarization pattern where the polarization is linear everywhere and rotates as a function of distance from the center [4]. Choosing the quantization axis to be along this polarization, molecules near zero velocity will be preferentially pumped into the $F = 2$, $m_F = \pm 2$ states, which have the least AC Stark shift and due to the red detuning, the highest energy [Fig. 1(d)]. As a consequence, when molecules move at low velocities in this laser configuration, they will constantly "roll down" a potential hill as they move through the corkscrew polarization, causing sub-Doppler heating [21]. With this picture in mind, the way to engineer the sub-Doppler force into a cooling force becomes straightforward. A far blue-detuned laser with the same polarization as the molasses beam can produce a larger AC Stark shift than the molasses beams, thereby changing the sign of the overall shift, resulting in cooling [Fig. 1(e)]. Due to its large detuning from resonance, this laser will not cause additional scattering forces, allowing for the Doppler cooling forces to remain intact. In reality the level structure of CaF is more complicated (Fig. 2). The $X^2\Sigma^+$ ground state consists of four hyperfine energy levels, $F = 1, 0, 1$, and 2, spaced by 76, 47, and 25 MHz. The $A^2\Pi_{1/2}$ excited state has a hyperfine splitting of 5 MHz. Four laser frequencies are used to drive transitions from the four ground states to the excited states, each detuned by $\delta = -\Gamma$ with respect to the $F' = 1$ excited state [20]. The lasers driving the $F = 1$ and $F = 0$ ground-state levels are σ^+ polarized whereas the one driving the $F = 2$ ground state is σ^- polarized. As such, the $F = 2$ to $F' = 1$ transition closely resembles the situation depicted in Fig. 1.

A full three-dimensional (3D) simulation of the 16-level optical Bloch equations (OBEs) for CaF using this laser configuration confirms our intuitive picture of optical pumping into the $m_F = \pm 2$ states. Our method for solving the OBEs is largely taken from Ref. [22], and we have verified that we can reproduce all results presented therein. The resulting velocity-dependent force is depicted as the blue curve in Fig. 3. The figure clearly shows the Doppler cooling and sub-Doppler heating features observed in experiment [7]. To get rid of this sub-Doppler heating, and perhaps even turn it into cooling, the $m_F = \pm 2$ states must be shifted down in energy instead of up, whereas not affecting the photon scattering much. This can be accomplished most easily with a laser detuned far into
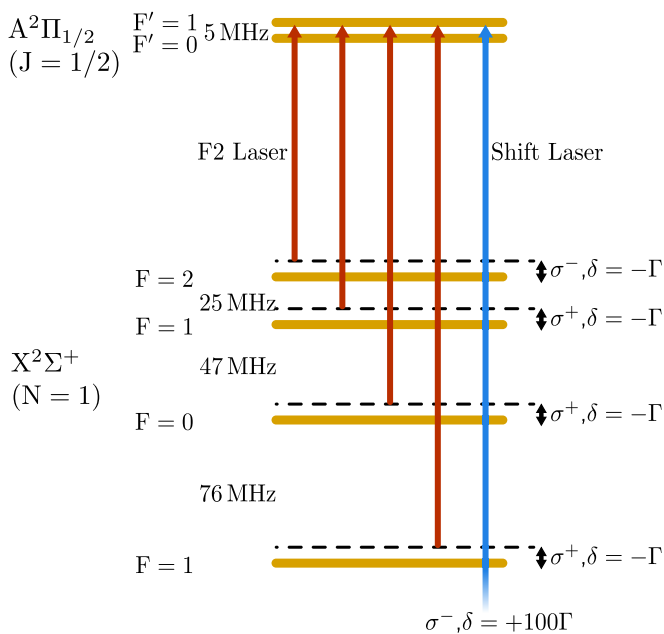
FIG. 2. Ground- and excited-state hyperfine levels of CaF and laser frequencies used to address them. The ground states are coupled to the excited states with four laser frequencies, each detuned by $\delta = -\Gamma$ from their respective transition. Also shown in blue is the shift laser, detuned by $\delta = +100\Gamma$ and with polarization equal to that of the F2 laser.
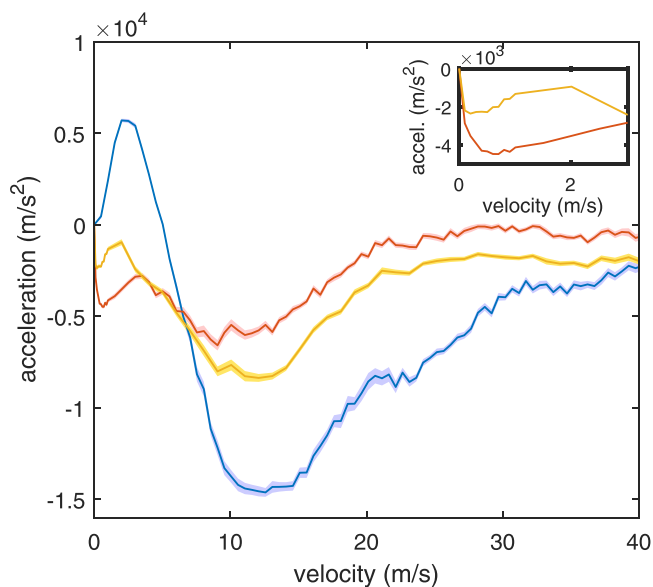

FIG. 3. Acceleration vs velocity for molecules in the MOT. The blue curve shows the acceleration in the usual four-laser component, dual-frequency MOTs used to date [22]. The red curve shows the acceleration when the blue-detuned shift laser is added with polarization equal to the $F = 2$ laser component, showing sub-Doppler cooling below 3 m/s. The yellow curve depicts the acceleration when the blue laser polarization is reversed with respect to the $F = 2$ component. The inset: closeup of the sub-Doppler cooling part of the red and yellow curves. Shaded areas reflect the 68% confidence intervals on the mean acceleration over 100 runs of the OBEs.

the blue. Because m_F is defined relative to the polarization of the most red-detuned frequency component (the one that is most responsible for optical pumping), this far off-resonant laser should have the same polarization as this component. For the rest of the discussion we will refer to this blue-detuned laser as the shift laser and to the most red-detuned laser as the F2 laser (see Fig. 2). For our simulations we choose a blue detuning of the shift laser of 100Γ (angular frequency), where $\Gamma = 2\pi \times 8.3$ MHz is the transition's natural linewidth. This detuning is large enough to ensure that the shift laser has little effect on the Doppler force (photon scattering), whereas being small enough to not cause any leakage to any states close by. The red curve in Fig. 3 shows the result of the OBEs when including this shift laser with a power of 80 mW and a Gaussian beam diameter of 4 mm. The other four, regular MOT frequency components share 200 mW of power and have a beam diameter of 20 mm. At these intensities, the shift laser introduces an AC stark shift on the $F = 2$ levels 0.6 times as large as that of the F2 laser. Together with the other three MOT frequencies, this shift is enough to reverse the AC stark shift caused by the F2 laser. The sub-Doppler heating which previously dominated the force for velocities below 6 m/s has disappeared, and in its place there is a sub-Doppler cooling force below 3 m/s. Applying the shift laser to the MOT, furthermore, seems to have reduced the Doppler force, presumably because the additional AC Stark shift has changed at what velocity the various ground states become resonant with the lasers, however, the force is still more than strong enough to keep the molecular cloud cold. A stronger shift laser would retain the sub-Doppler cooling, but would eventually flip the sign of the Doppler force. Whereas this

may be counteracted by changing the detunings of the MOT lasers, such an optimization is beyond the scope of this paper. Due to the smaller diameter of the shift laser beam (4 mm) as compared to the MOT beams (20 mm) the capture velocity of the MOT should remain largely unchanged. Alternatively, one could switch on the shift laser after MOT loading as an additional compression/cooling step. The effect of the shift laser on the trapping force is shown in Fig. 4. A blue-detuned laser can, in principle, result in a repulsive force, but this effect is negligible for our parameters as can be seen from the figure. Since the radius of the shift laser is chosen to be 2 mm the figure only shows the acceleration for positions up to 3 mm. Calculating the trapping force using the OBEs needs a lot of averaging [22] as it fluctuates a lot depending on the initial conditions chosen. As such, whereas the red curve in Fig. 4 seems to show a small force at the MOT center, our uncertainty in the calculation is consistent with zero force, and we force it to be so in our further modeling.

The requirement that the shift laser has the same polarization as the F2 laser translates to the condition that the phase of the σ^+ and σ^- parts should be the same over the size of the MOT. This results in two constraints for experiments (see Appendix A): the red and blue components must be co-propagating from the point on where their σ^+ and σ^- beams are split, and the path length difference between counterpropagating beams must be an integer multiple of the beat length between the F2 and shift lasers. The former constraint is necessary for the polarization gradients of the two components to remain in-phase with each other. The latter constraint
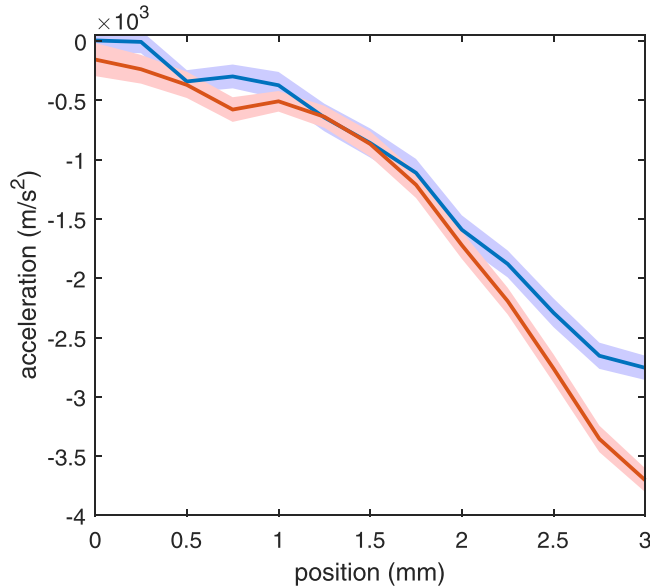
FIG. 4. Acceleration vs position for molecules in the MOT. The blue curve shows the acceleration in the usual four-laser component, dual-frequency MOTs used to date [22]. The red curve shows the acceleration when the blue-detuned shift laser is added with polarization equal to the $F = 2$ laser component. Adding the extra blue laser seems to have little effect on the trapping force. Shaded areas indicate the 68% confidence intervals of acceleration for 1000 runs of the OBEs.
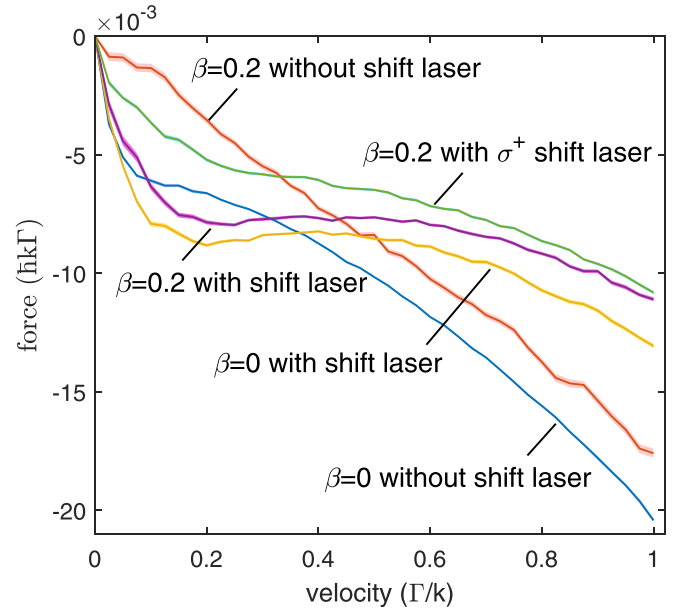

FIG. 5. Velocity-dependent force for a $F = 1$ to $F' = 2$ system in a 3D MOT as a function of the magnetic-field $B = \beta \hbar \Gamma / \mu_B$. Parameters for the MOT laser are $I = I_{sat}$, $\delta = -2.5\Gamma$. Parameters for the shift laser are $I = 80 I_{sat}$, $\delta = -40\Gamma$. The polarization of the laser beams coming from the positive direction is σ^- unless specified. The g factors of both the ground and excited states are 1. Shaded areas indicate the 68% confidence intervals of acceleration for 500 runs of the OBEs.

ensures that the polarization direction of the two components is the same over the size of the MOT. For the detuning chosen in our simulations, this constrains the path-length difference between counterpropagating beams to multiples of 36 cm with a tolerance of 1 cm to keep the angle between F2 and shift laser polarization below 5°. Both constraints should be readily realizable in experiments. The yellow curve in (Fig. 3) shows what happens to the acceleration when the polarization of the shift laser is reversed (i.e., σ^+ turned to σ^- and vice versa). This causes the polarizations of the shift and F2 lasers to not be equal at every point in space anymore, significantly reducing the sub-Doppler cooling. There does remain a small cooling feature, however, and as such, the shift laser should help improve MOT temperatures and densities even when the above two constraints are not met.

Using our results from the OBEs we can estimate the temperatures and densities the sub-Doppler cooling MOT should be capable of reaching. To this end, we perform a simple Monte Carlo simulation (see Appendix A). From the velocity distribution obtained this way (see Fig. 7 in Appendix A) we estimate the MOT temperature to be $40\,\mu K$, well below the Doppler limit of $\approx 200\,\mu K$ [6]. Similarly low MOT temperatures have previously been observed in experiment for blue-detuned MOTs of atoms [13,23], whereas current dual-frequency CaF MOTs only reach temperatures of about 1 mK, and, consequently, densities on the order of $1 \times 10^6\,cm^{-3}$ [24]. Whereas experiments can lower the temperature of these MOTs by decreasing laser intensities, this comes at the cost of a further reduction in MOT density [6]. The peak density of our MOT is simulated to be $4 \times 10^8\,cm^{-3}$ for 1×10^5

molecules, a value much higher than current molecular MOTs are capable of reaching. It should be noted that the density is limited, in part, by our choice of magnetic-field gradient ($15\,G/cm$) and higher densities may be reached by increasing this value.

Lastly, to show that the ideas presented here can intuitively be applied to a variety of systems, we use them here to engineer a MOT for atoms with robust sub-Doppler cooling. In normal atomic MOTs, sub-Doppler cooling features exist, but they are quickly destabilized by Zeeman shifts, and can essentially be ignored. By using a shift laser, however, it should be possible to produce AC Stark shifts great enough to overcome Zeeman shifts and extend the range of sub-Doppler cooling at the MOT center. To demonstrate this, we use the OBEs to model a simple type-I $F = 1$ to $F' = 2$ system with MOT lasers of intensity $I = I_{sat}$, the saturation intensity, and detuning $\delta = -2.5\Gamma$ in a magnetic field (Fig. 5). The field strength β is given in units of $\hbar \Gamma / \mu_B$ as was performed in Ref. [21]. The large slope near zero velocity can be attributed to sub-Doppler cooling. As was already seen in Ref. [21], sub-Doppler cooling has already completely disappeared at a field of $\beta = 0.2$, corresponding to $\approx 1\,G$ for a typical alkali atom. At this field, the "$\beta = 0.2$ without the shift laser" line in Fig. 5 shows no sub-Doppler "bump" and simply follows a Lorentzian lineshape at higher velocities as is expected for the Doppler force. To regain sub-Doppler cooling in this type-I system, a red-detuned shift laser with the same polarization as the MOT lasers should be used. Adding such a laser with an intensity of $80 I_{sat}$ and detuning of $\delta = -40\Gamma$, we see that the sub-Doppler cooling range extends to, at least, a field of

$\beta = 0.2$. Our simulations show that sub-Doppler forces persist even at $\beta = 0.8$. As was the case with the molecular MOT, reversing the polarization of this laser significantly reduces its effects.

In conclusion, we have shown that it is possible to engineer sub-Doppler forces inside a magneto-optical trap using far off-resonant laser beams and a careful choice of polarization. Using this principle we designed a MOT for CaF molecules with sub-Doppler cooling and estimated that it should reach temperatures of $40\,\mu$K and densities of 4×10^8 cm^{-3} for 10^5 molecules. Such densities are much larger than is currently being reached in molecular CaF MOTs [18], and they are a direct consequence of the lower MOT temperature. The low temperature and high density result in a phase-space density of our simulated MOT of 2×10^{-8}. Whereas this paper has concentrated on improving molecular magneto-optical traps, the idea that AC Stark shifts, and as such, sub-Doppler effects, can be engineered is quite general. We have shown that the same ideas can be used to engineer an atomic MOT with robust sub-Doppler cooling at its center. If such a MOT is capable of producing colder denser samples than current atomic MOTs are capable of, it may be used to directly load optical dipole traps, improving the way to all-optical BECs of (for example) alkali atoms. We expect many uses for the technique across the broad spectrum of atom and molecular physics experiments being performed today.

APPENDIX A: MONTE CARLO SIMULATION

Here we present the details of our Monte Carlo simulation. The optical Bloch equations are solved to find the damping and trapping forces, closely following the method outlined in Ref. [22]. To account for the effects of vibrational repumping, we reduce all forces by a factor of 2. For simplicity we use the axial 1D trapping force with the shift laser present and ignore the fact that the MOT is weaker in the radial direction. We calculate the velocity damping force as well as the probability of being in the excited state for velocities up to $4\Gamma/k$ and positions up to 3 mm (Fig. 6). Here, Γ is the natural linewidth of the transition, and k is the magnitude of the wave vector. Since the shift laser beam diameter is smaller than the other MOT lasers, we see a transition from sub-Doppler cooling to sub-Doppler heating at larger positions. Even though our initial cloud size overlaps significantly with the heating region, the final MOT size is smaller than the shift laser beam so that the heating does not affect the final cloud temperature. For the trapping force, we make the approximation that its dependence on the velocity is negligible and use the force in Fig. 4. As is stated in the main text, the force in Fig. 4 has a small value at the MOT center, which would be unphysical. Our error estimates show that this value is consistent with zero, however, and we set it to zero for our simulations.

We start the simulation with a uniform 3D distribution of 10^4 molecules with a radius of 3 mm. The 3D velocity distribution is also chosen to be uniform with a radius of 1 m/s.
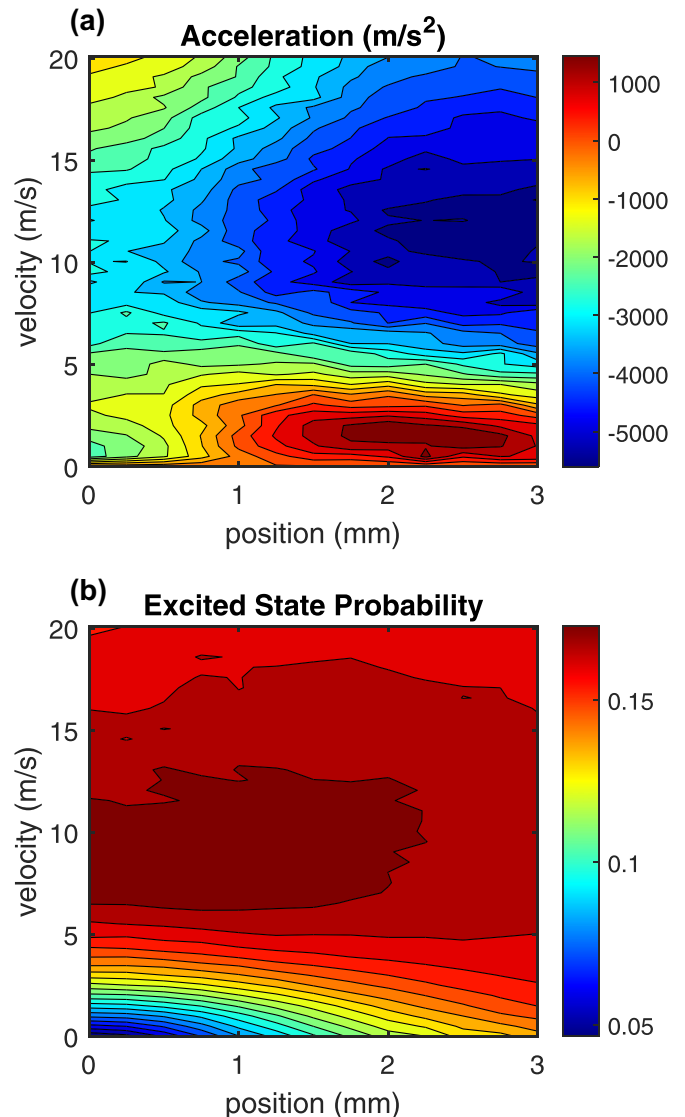

FIG. 6. Velocity damping force (acceleration) (a) and excited state probability (b) of the molecules vs position and velocity in the MOT.

Because the profiles in Figs. 4 and 6 are relatively coarse, we use linear interpolation of their data to calculate the force at the velocity and position of each molecule. Photon scattering is included as momentum kicks of $\hbar k$ in a random direction with a probability of $\Gamma\rho_{ee}dt$, where ρ_{ee} is the excited-state probability and dt is the time step of the calculation. In case this probability exceeds 1, we instead give the molecule a momentum kick of $\sqrt{\Gamma\rho_{ee}dt}$ every time step. Time steps in the simulation are chosen to switch periodically between $100/\Gamma$ and $1/\Gamma$. The $100/\Gamma$ steps allow for the molecules to propagate in space whereas keeping the computation time reasonable, whereas the $1/\Gamma$ steps more accurately model photon scattering. For the final time evolution we give 10^6 steps of $1/\Gamma$ to make sure equilibrium is reached. The resulting velocity and radial position distributions are plotted in Fig. 7. From these we extract a temperature of $40\,\mu$K using $T = mv_{rms}^2/3k_B$. This temperature is the result of a balancing of the sub-Doppler cooling force and residual heating from
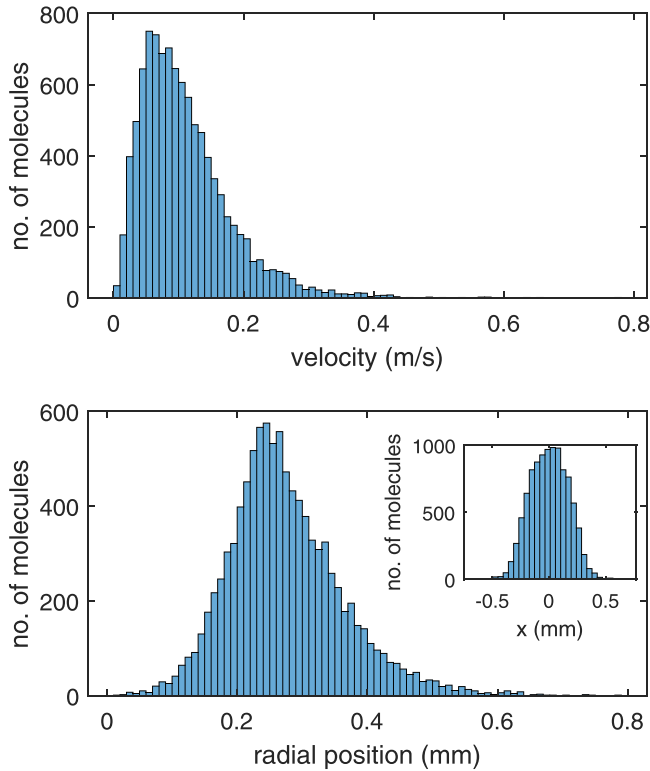
FIG. 7. Distribution of velocities and radial positions of 10^4 molecules subjected to the forces given in Figs. 4 and 6. The inset shows the 1D distribution of molecules along one of the Cartesian coordinates.

photon scattering due to the nonzero excited-state probability near $v = 0$ m/s. The central density is calculated by simply counting the number of molecules in a $0.3 \times 0.3 \times 0.3$ mm^3 cube in the center of the cloud.

APPENDIX B: REQUIREMENTS ON RED AND BLUE LASER COMPONENTS

For the conventional MOT, at low velocities, molecules are optically pumped by the red most laser component (F2 laser), which forms a corkscrew polarization pattern in space. Choosing the quantization axis along the local polarization of this laser, the OBEs confirm that molecules are pumped into

the $m_F = \pm 2$ ground-state levels, which are dark states to this laser. In order for our scheme to produce sub-Doppler cooling, our blue AC Stark shift laser must shift the $m_F = \pm 1$ and $m_F = 0$ levels above the $m_F = \pm 2$ levels, and as such it needs the same local linear polarization as the F2 laser. Two conditions can be derived from this requirement. First, whereas it is okay that the local polarization changes in time (due to, e.g., vibrations of the mirrors), the corkscrews produced by the blue and red lasers must not dephase with respect to one another. The easiest way to achieve this in experiment is to have both lasers overlap from the moment that the σ^+ and σ^- components are split. This way, any phase induced by vibrations will be placed on both beams and their polarizations will rotate together. Even with the blue and red lasers taking the same path, there is a second requirement: if the arm lengths for the σ^+ and σ^- beams are the same there will be zero phase difference between them when they meet in the MOT center. If the arm length is different, however, the phase between σ^+ and σ^- will be given by

$$\Delta\theta = k(z_+ - z_-) = k\,\Delta z, \qquad (B1)$$

where k is the wave vector and z_+ and z_- are the path lengths for the σ^+ and σ^- components, respectively. Because the shift and F2 lasers have different wave vectors, this phase is not necessarily the same for them, causing their linear polarizations to be at an angle with respect to each other. This phase difference, then, is given by

$$\Delta\phi = \Delta k\,\Delta z = \frac{2\pi(f_b - f_r)}{c}\Delta z = \frac{100\Gamma}{c}\Delta z, \qquad (B2)$$

using the detuning we have chosen for the shift laser in our simulations. From this, using the excited-state linewidth of CaF, we see that the path-length difference between counterpropagating MOT beams should be multiples of 36 cm. If we allow for a $5°$ angle between the polarizations of the red and blue beams we may have a path-length difference uncertainty of ± 1 cm.

Making sure that each counterpropagating MOT pair travels the same distance ± 1 cm should certainly be possible in experiments. If, on the other hand, one wants to use a single laser to produce all six MOT beams in order to not split power into multiple paths, care must be taken that each retroreflected beam has traveled multiples of 36 cm, a number that also seems reasonable.

[1] E. L. Raab, M. Prentiss, A. Cable, S. Chu, and D. E. Pritchard, Trapping of Neutral Sodium Atoms with Radiation Pressure, Phys. Rev. Lett. **59**, 2631 (1987).

[2] C. Monroe, W. Swann, H. Robinson, and C. Wieman, Very Cold Trapped Atoms in a Vapor Cell, Phys. Rev. Lett. **65**, 1571 (1990).

[3] P. D. Lett, R. N. Watts, C. I. Westbrook, W. D. Phillips, P. L. Gould, and H. J. Metcalf, Observation of Atoms Laser Cooled below the Doppler Limit, Phys. Rev. Lett. **61**, 169 (1988).

[4] J. Dalibard and C. Cohen-Tannoudji, Laser cooling below the Doppler limit by polarization gradients: simple theoretical models, J. Opt. Soc. Am. B **6**, 2023 (1989).

[5] D. S. Weiss, E. Riis, Y. Shevy, P. J. Ungar, and S. Chu, Optical molasses and multilevel atoms: experiment, J. Opt. Soc. Am. B **6**, 2072 (1989).

[6] S. Truppe, H. J. Williams, M. Hambach, L. Caldwell, N. J. Fitch, E. A. Hinds, B. E. Sauer, and M. R. Tarbutt, Molecules cooled below the doppler limit, Nat. Phys. **13**, 1173 (2017).

[7] L. Anderegg, B. L. Augenbraun, Y. Bao, S. Burchesky, L. W. Cheuk, W. Ketterle, and J. M. Doyle, Laser cooling of optically trapped molecules, Nat. Phys. **14**, 890 (2018).

[8] S. Ding, Y. Wu, I. A. Finneran, J. J. Burau, and J. Ye, Sub-Doppler Cooling and Compressed Trapping of

YO Molecules at μK Temperatures, Phys. Rev. X **10**, 021049 (2020).

[9] H. F. Hess, Evaporative cooling of magnetically trapped and compressed spin-polarized hydrogen, Phys. Rev. B **34**, 3476 (1986).

[10] M. H. Anderson, J. R. Ensher, M. R. Matthews, C. E. Wieman, and E. A. Cornell, Observation of Bose-Einstein condensation in a dilute atomic vapor, Science **269**, 198 (1995).

[11] K. B. Davis, M. O. Mewes, M. R. Andrews, N. J. van Druten, D. S. Durfee, D. M. Kurn, and W. Ketterle, Bose-Einstein Condensation in a Gas of Sodium Atoms, Phys. Rev. Lett. **75**, 3969 (1995).

[12] W. Ketterle and N.J. Van Druten, *Evaporative Cooling of Trapped Atoms* (Academic Press, 1996), pp. 181–236

[13] K. N. Jarvis, J. A. Devlin, T. E. Wall, B. E. Sauer, and M. R. Tarbutt, Blue-Detuned Magneto-Optical Trap, Phys. Rev. Lett. **120**, 083201 (2018).

[14] C. J Cooper, G. Hillenbrand, J. Rink, C. G Townsend, K. Zetie, and C. J Foot, The temperature of atoms in a magneto-optical trap, Europhys. Lett. **28**, 397 (1994).

[15] H. J. Williams, S. Truppe, M. Hambach, L. Caldwell, N. J. Fitch, E. A. Hinds, B. E. Sauer, and M. R. Tarbutt, Characteristics of a magneto-optical trap of molecules, New J. Phys. **19**, 113035 (2017).

[16] J. F. Barry, D. J. McCarron, E. B. Norrgard, M. H. Steinecker, and D. DeMille, Magneto-optical trapping of a diatomic molecule, Nature (London) **512**, 286 (2014).

[17] A. L. Collopy, S. Ding, Y. Wu, I. A. Finneran, L. Anderegg, B. L. Augenbraun, J. M. Doyle, and J. Ye, 3D Magneto-Optical Trap of Yttrium Monoxide, Phys. Rev. Lett. **121**, 213201 (2018).

[18] L. Anderegg, B. L. Augenbraun, E. Chae, B. Hemmerling, N. R. Hutzler, A. Ravi, A. Collopy, J. Ye, W. Ketterle, and J. M. Doyle, Radio Frequency Magneto-Optical Trapping of CaF with High Density, Phys. Rev. Lett. **119**, 103201 (2017).

[19] A. M. L. Oien, I. T. McKinnie, P. J. Manson, W. J. Sandle, and D. M. Warrington, Cooling mechanisms in the sodium type-ii magneto-optical trap, Phys. Rev. A **55**, 4621 (1997).

[20] M. R. Tarbutt and T. C. Steimle, Modeling magneto-optical trapping of caf molecules, Phys. Rev. A **92**, 053401 (2015).

[21] J. A. Devlin and M. R. Tarbutt, Three-dimensional doppler, polarization-gradient, and magneto-optical forces for atoms and molecules with dark states, New J. Phys. **18**, 123017 (2016).

[22] J. A. Devlin and M. R. Tarbutt, Laser cooling and magneto-optical trapping of molecules analyzed using optical bloch equations and the fokker-planck-kramers equation, Phys. Rev. A **98**, 063415 (2018).

[23] B. Piest, V. Vollenkemper, J. Böhm, A. Herbst, and E. M. Rasel, Red- and blue-detuned magneto-optical trapping with liquid crystal variable retarders, Rev. Sci. Instrum. **93**, 023202 (2022).

[24] H. J. Williams, L. Caldwell, N. J. Fitch, S. Truppe, J. Rodewald, E. A. Hinds, B. E. Sauer, and M. R. Tarbutt, Magnetic Trapping and Coherent Control of Laser-Cooled Molecules, Phys. Rev. Lett. **120**, 163201 (2018).